



Cite this: DOI: 10.1039/d0nj05101b

Fabrication of porous ultrathin carbon nitride nanosheet catalysts with enhanced photocatalytic activity for N- and O-heterocyclic compound synthesis†

Yancong Li, Jiliang Ma, * Zhendong Liu, Dongnv Jin, Gaojie Jiao, Yanzhu Guo, Qiang Wang, Jinghui Zhou and Runcang Sun*

A simple and efficient photocatalytic method for the synthesis of dihydropyrimidinones (DHPMs) and their derivatives *via* porous ultrathin carbon nitride nanosheets (p-CNNs) without solvents was demonstrated. The yields of 3,4-dihydropyrimidin-2(1*H*)-ones/thiones and their derivatives were up to 97.0%. Furthermore, the yield of 5-ethoxycarbonyl-6-methyl-4-phenyl-3,4-dihydropyrimidin-2(1*H*)-one in the 10th cycle retained 98.9% of its 1st value. Considering the environmental and economic benefits, this work exhibits various merits including excellent yields, environmental friendliness, inexpensiveness, and avoiding the use of solvents and metal-based photocatalysts. In addition, the excellent performance of the p-CNNs and environmentally benign reaction system have also been checked by the photocatalytic synthesis of 12-phenyl-9,9-dimethyl-8,9,10,12-tetrahydrobenzo[*a*]xanthen-11-one and 5-phenyl-1(4-methoxyphenyl)-3[(4-methoxy-phenyl)-amino]-1*H*-pyrrol-2(5*H*)-one. This work paves a new way for carrying out a three-component reaction using metal-free photocatalysts under mild reaction conditions.

 Received 17th October 2020,
 Accepted 18th November 2020

DOI: 10.1039/d0nj05101b

rsc.li/njc

Introduction

Green organic synthesis has become a matter of great concern in recent years. To achieve this goal, various strategies have been developed involving three criteria: solvent, catalyst, and synthesis method.^{1–3} Photocatalysis as a green synthesis method has attracted much attention due to its high efficiency, easy operation, mild reaction conditions, wide application, low cost, low energy consumption and so on.^{4–6} The key to proper design of a photocatalytic reaction is to first design and prepare an appropriate photocatalyst. The traditional photocatalysts, such as metal oxides (ZnO, TiO₂)^{7,8} and metal sulfides (CdS, ZnS),^{9,10} exhibited high photocatalytic performance. However, some of them suffered from the narrow absorption range of visible light or light corrosion, which limited their application. Recently, a series of novel photocatalysts have been reported, such as BiOX (X = Cl, Br, I), metal-organic frameworks (MOFs), covalent organic frameworks (COFs) or functional carbon nitride.^{11–16} These functionalized photocatalysts have made great achievements in the fields of solar water splitting,¹⁴ CO₂ reduction,^{17–19} N₂ fixation,²⁰ biorefinery²¹ and

organic synthesis.²² High cost and complex preparation processes of other photocatalysts as compared with functional carbon nitride development requirements. Thus, taking environmental and economic benefits into consideration, the development of various metal-free, environmentally friendly and inexpensive functional carbon nitride photocatalysts for use in organic synthesis is of great significance.

Dihydropyrimidinones (DHPMs) and their derivatives are a series of heterocyclic compounds, which are widely distributed in nature. Since the DHPMs were discovered, they have attracted much attention due to their wide range of biological activities, such as antiviral, antimitotic, anticarcinogenic and antihypertensive effects.^{23–25} Furthermore, some functionalized DHPMs are the constituents of neuropeptide Y antagonists, calcium channel modulators and α -1a antagonists.^{26–28} Especially Batzelladine A and B play an important role in the HIV gp-120-CD4 treatment.²⁹ Therefore, developing a mild and efficient strategy is significant for the synthesis of DHPMs.

The first straightforward method for the synthesis of DHPMs *via* condensation of aldehydes, β -dicarbonyl compounds and urea or thiourea reported by P. Biginelli (the reaction was then named as Biginelli reaction)³⁰ inspired a new wave of research on the synthesis and application of DHPMs. And after that, various strategies for carrying out Biginelli reaction were developed.^{31–36} However, most of them suffered from longer reaction time,

Center for Lignocellulosic Chemistry and Biomaterials, College of Light Industry and Chemical Engineering, Dalian Polytechnic University, Dalian, 116034, China.
 E-mail: jlma@dlpu.edu.cn, rcsun3@dlpu.edu.cn

† Electronic supplementary information (ESI) available. See DOI: 10.1039/d0nj05101b

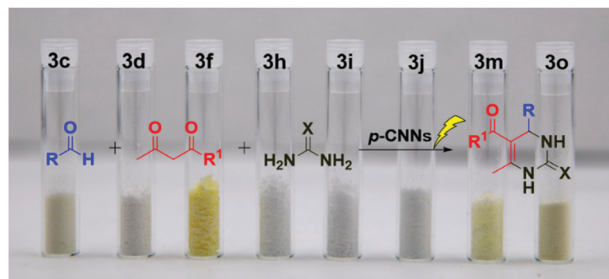
harsher reaction conditions, high cost, and tedious work-up or purification. Currently, several new protocols with natural catalysts (e.g. citric acid,³⁷ baker's yeast,³⁸ phytic acid,³⁹ D-xylonic acid,² etc.) for carrying out Biginelli reaction have been demonstrated, which gave good yields. The only problem is that the recovery and reuse of these catalysts are relatively complicated. In this regard, efficient heterogeneous catalysts have aroused great interest among researchers. Taking into account the advantages of photocatalysis, developing a metal-free and efficient heterogeneous photocatalyst for carrying out Biginelli reaction has vital significance.

In this study, p-CNN photocatalyst was prepared by direct calcination of copper oxide nanobelts (CuO NBs) and melamine, which could effectively synthesize 3,4-dihydropyrimidin-2(1H)-ones/thiones and their derivatives photocatalytically without solvents under mild conditions (Scheme 1). The performance of p-CNNs in the photothermal mediated Biginelli reaction was assessed at varying irradiation time (30–120 min), temperature (30–100 °C), photocatalyst dosage (0.56–5.60 wt%) and feed ratios. Furthermore, the stability and recycling of p-CNNs were also investigated. In addition, the excellent performance of p-CNNs and the environmentally benign reaction system were also checked by the photocatalytic synthesis of 12-phenyl-9,9-dimethyl-8,9,10,12-tetrahydrobenzo[a]xanthen-11-one and 5-phenyl-1(4-methoxyphenyl)-3[(4-methoxyphenyl)-amino]-1H-pyrrol-2(5H)-one (Schemes 2 and 3).

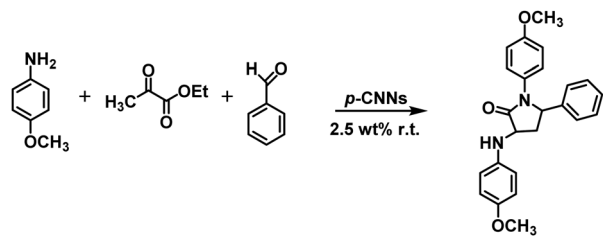
Experimental section

Materials

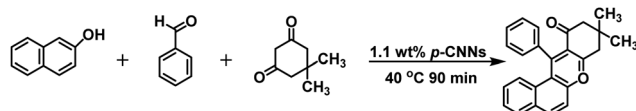
Melamine, sodium hydroxide, cetyltrimethylammonium bromide and copperdiacetatehydrate were provided by Macklin



Scheme 1 p-CNNs photocatalytic synthesis of DHPMs under solvent-free conditions.



Scheme 2 Photocatalytic p-CNNs for the synthesis of 5-phenyl-1(4-methoxyphenyl)-3[(4-methoxyphenyl)-amino]-1H-pyrrol-2(5H)-one under solvent-free conditions.



Scheme 3 p-CNNs photocatalytic for the synthesis of 12-phenyl-9,9-dimethyl-8,9,10,12-tetrahydrobenzo[a]xanthen-11-one under solvent-free conditions.

Industrial Corporation (Shanghai, China). Aldehydes and 1,3-dicarbonyl compounds were purchased from Aladdin Industrial Corporation. Urea, thiourea, ethanol and other reagents were obtained from Dalian Chemical Reagent Factory, China. All the chemicals were analytical grade and used directly without further purification.

Preparation of photocatalyst

In a typical procedure, a certain amount of sodium hydroxide (NaOH) was dissolved in a certain volume of deionized water under ice water bath. Subsequently, cetyltrimethylammonium bromide (CTAB) was added into the above solution with a mass ratio of 1:5.5 (CTAB:NaOH). The system was then heated from room temperature to 60 °C under stirring to give a NaOH–CTAB solution. In addition, a certain amount of copperdiacetatehydrate was dissolved in deionized water, and the solution was then added into the NaOH–CTAB solution drop by drop. The obtained mixed system was heated at 60 °C for 60 min. After the reaction was complete, the reaction system was filtered while hot and washed three times with deionized water and ethanol, respectively. The black solid products were dried at 50 °C for 12 h. Finally, the CuO NB was calcined at 350 °C for 120 min under N₂ atmosphere before use.

The method for the preparation of multilayer carbon nitride (ml-CN) was based on the reported literature,⁴⁰ with a slight difference. First, 2.0 g of melamine and 3 mL of deionized water were taken in a crucible; the mixed system was then stirred for 30 min. Subsequently, the mixture was calcined at 250 °C for 60 min under N₂ atmosphere. After the calcination process was complete, the system was heated to 560 °C with a rate of 5 °C min⁻¹ and then kept for 180 min. The obtained ml-CN powder was calcined at 560 °C for another 115 min before use.

In a typical procedure: first, 2.0 g of melamine, 10 mg of CuO NB and 3 mL of deionized water were taken in a crucible; the mixed system was then stirred for 30 min. Subsequently, the mixture was calcined at 250 °C for 60 min under N₂ atmosphere. After the calcination process was complete, the system was heated to 560 °C with a rate of 5 °C min⁻¹ and then kept for 180 min. The obtained powder was fully ground and then calcined at 560 °C for 115 min under N₂ atmosphere to give p-CNNs.

Characterization

The investigation of morphology by scanning electron microscopy (SEM), transmission electron microscopy (TEM) and atomic force microscopy (AFM) was conducted on Hitachi-4800 SEM, Nano-scope III AFM and JEM-2100 CXII TEM, respectively. X-ray photoelectron spectroscopy (XPS) was studied using a Kratos Axis Ultra DLD spectrometer equipped with a monochromatic AlK_α X-ray

source. X-ray diffraction (XRD) patterns of the ml-CN and p-CNNs were explored by a Bruker D8 Focus diffractometer. Fourier transform infrared (FT-IR) spectra of the catalysts were investigated by a Bruker Tensor 27 spectrophotometer in the range of 400–4000 cm^{-1} . N_2 adsorption–desorption isotherm measurements were conducted using a physisorption analyzer, and the Brunauer–Emmett–Teller (BET) method was used to calculate the specific surface area, as well as the desorption branch of the isotherm in line with the Barrett–Joyner–Halenda method was utilized to evaluate the average pore diameter and pore size distribution of p-CNNs. The ultraviolet-visible diffuse reflectance spectra (UV-vis DRS) of ml-CN and p-CNNs were recorded on a Cary 5000 spectrophotometer fitted with an integrating sphere attachment from 200 to 800 nm. Inductively coupled plasma atomic emission spectroscopy (ICP-MS) was performed using an Agilent 7800 equipment. ^1H NMR spectral measurements were performed at 400 MHz using TMS as the internal standard, and ^{13}C NMR spectral measurements were carried out at 100 MHz with complete proton decoupling.

General procedure for the synthesis of dihydropyridine-2(1H)-ones/thiones by using p-CNN photocatalyst

In a typical procedure, a mixture of aldehydes, 1,3-dicarbonyl compounds, urea or thiourea and p-CNNs was added into a reactor. The mixture was stirred at dark condition for 30 min. Subsequently, the reaction system was conducted at different temperatures for different irradiation time. Once the reaction was complete, ice water was added. The obtained crude product was then washed with ice water several times, filtered and dried at 100 °C for 10 h. Finally, the pure products were obtained by recrystallization of the crude products in ethanol.

In the cycling experiment, the p-CNNs was recovered during the recrystallization process. The obtained p-CNNs was washed with hot ethanol several times and then dried at 100 °C for 10 h before reuse.

General procedure for the synthesis of 12-phenyl-9,9-dimethyl-8,9,10,12-tetrahydrobenzo[*a*]xanthen-11-one using p-CNN photocatalyst

In a typical procedure, a mixture of benzaldehyde (1.0 mmol), 2-naphthol (1.0 mmol), trimethadione (1.2 mmol) and p-CNNs (1.1 wt%) was added into a reactor. The mixture was stirred at dark condition for 30 min. Subsequently, the reaction system was performed at 40 °C for 90 min under visible-light irradiation. Once the reaction was complete, the system was cooled to room temperature and ethyl acetate was added. The reaction system was then filtered and washed with ethyl acetate several times, and the obtained filtrate was collected. The pure product was afforded by evaporation of the collected filtrate, followed by column chromatography on silica gel using ethyl acetate/petroleum ether as the eluent.

General procedure for the synthesis of 5-phenyl-1(4-methoxyphenyl)-3[(4-methoxyphenyl)-amino]-1H-pyrrol-2(5H)-one by using p-CNN photocatalyst

In a typical procedure, a mixture of benzaldehyde (1.0 mmol), *p*-methoxyaniline (2.0 mmol), ethyl pyruvate (1.5 mmol) and

p-CNNs (2.5 wt%) was added into a reactor. The mixture was stirred at dark condition for 30 min. Subsequently, the reaction system was performed at room temperature for 0.5 h under visible-light irradiation. Once the reaction was complete, 5 mL of ethanol was added and the obtained reaction system was stirred for 3–4 min. Subsequently, the reaction system was filtered and washed with ethanol and ether several times, respectively. The pure product was finally obtained by drying at 80 °C for 10 h.

Results and discussion

The characterization of samples

The morphology of ml-CN and p-CNNs was investigated by scanning electron microscopy (SEM), transmission electron microscopy (TEM) and atomic force microscopy (AFM). The ml-CN prepared by the direct calcination of the melamine slurry without the addition of CuO NB displayed obvious multi-layer structure (Fig. 1A), while the p-CNNs prepared by the simple calcination of CuO NB (Fig. S1, ESI[†]) and melamine exhibited typical two-dimensional structure (Fig. 1B). This finding shows that CuO NB can assist the p-CNNs to form nanosheet structure during the calcination process. The lamellar structure and amorphous structure of the p-CNNs was also observed by TEM results, as well as the amounts of holes existing in the nanosheet (Fig. 1C and D). To further investigate the porous structure of p-CNNs, AFM measurement was performed, and the obvious pores were found (Fig. 1E). Meanwhile, the p-CNN was hundreds of nanometers in width and ~1.5 nm in thickness (Fig. 1F). All the results indicated that the p-CNNs prepared in this work owns porous and flaky structure, which is beneficial for the adsorption and mass transfer of the reactants.

To investigate the chemical composition and status of the elements in p-CNNs, XPS measurement was carried out. As shown in Fig. 2A, three peaks were observed in the C 1s spectra, which were located at 288.3 eV, 286.5 eV and 284.8 eV, corresponding to N = C–N, C–N and C–C, respectively.⁴¹ The narrow scan N 1s spectra of p-CNNs are shown in Fig. 2B, and the peaks were observed at 401.4 eV, 400.3 eV and 398.8 eV, attributed to N–C, N–(C)₃ and C–N=C, respectively.⁴² Meanwhile, no Cu related species were detected in the XPS spectra. Furthermore, the results of ICP-MS show that there is no Cu loading in the p-CNNs. Fig. 2C displays the XRD patterns of ml-CN and p-CNNs, which is similar to that of pure graphitic carbon nitride (JCPDS Card No. 87-1526). The only difference is that the intensity of the (100) and (002) planes of p-CNNs was lower than that of ml-CN, leading to the reduction of interlayer distance of the graphitic like planar p-CNNs. As shown in Fig. 2D, the FT-IR spectra of ml-CN and p-CNNs were similar with those reported;⁴³ besides the change in signal peak intensity, no obvious difference in the FT-IR spectra of ml-CN and p-CNNs was observed. The N_2 sorption isotherms of p-CNNs exhibited type IV isotherm patterns, suggesting that lots of mesopores exist in p-CNNs, and the surface area was 85.2 $\text{m}^2 \text{g}^{-1}$ (Fig. 2E). To investigate the visible-light absorption regions of ml-CN and p-CNNs, UV-vis DRS was performed. As shown in Fig. 2F, the spectrum of the sample showed blue-shift with the

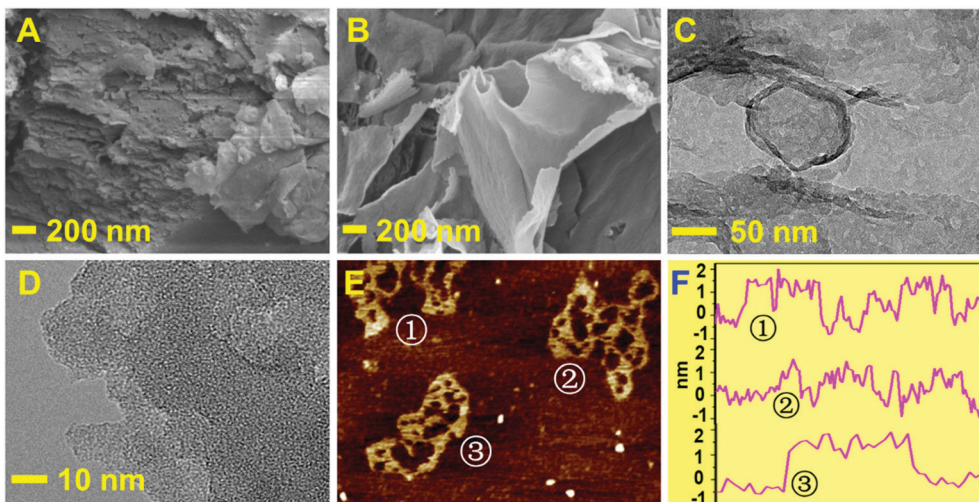


Fig. 1 SEM images of ml-CN (A) and p-CNNs (B); TEM images of p-CNNs (C and D); AFM images of p-CNNs (E) and its thickness distribution curves (F).

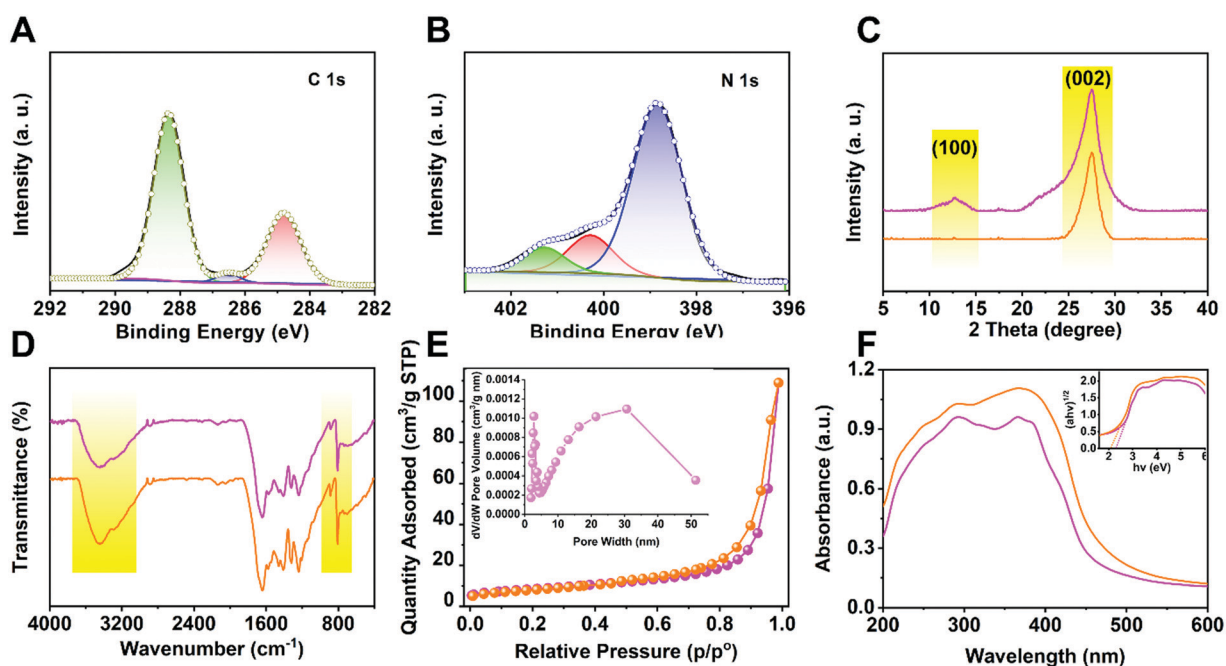


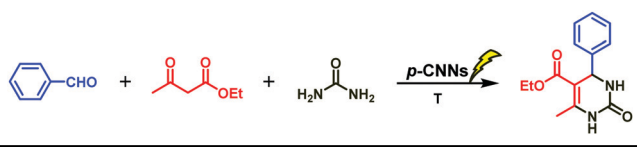
Fig. 2 XPS spectra of p-CNNs, (A): C 1s, (B): N 1s; (C): XRD patterns of ml-CN (magenta) and p-CNNs (orange); (D): FT-IR spectra of ml-CN (magenta) and p-CNNs (orange); (E): N₂ adsorption isotherm, inset in E shows the BJH pore size distribution; (F): UV-vis DRS of ml-CN and p-CNNs, inset in F shows the plot of transformed Kubelka–Munk function versus photo energy for ml-CN and p-CNNs.

decrease of thickness, indicating that the excitations by photo-carriers with energy is lower as compared with the intrinsic band-band transition. Furthermore, their bandgaps reduced with the decrease in sample thickness, resulting in an enhanced photocatalytic activity.

The photocatalytic activity of samples

Initially, the influence of visible light or dark condition on Biginelli reaction catalyzed by p-CNNs was investigated. The product of the Biginelli condensation reaction of benzaldehyde (5 mmol) with ethyl acetoacetate (5 mmol) and urea (5 mmol)

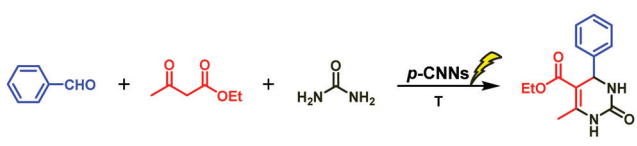
was named as **3a**. When the reaction catalyzed by p-CNNs was carried out at 40 °C or 90 °C for 60 min in the dark conditions, only trace amounts of **3a** was obtained. Once visible light was applied in the above system at 40 °C, 19.0% yield of **3a** was observed, suggesting that visible light is beneficial for the synthesis of **3a**. Subsequently, the effects of reaction time and reaction temperature on the synthesis of **3a** photocatalyzed by p-CNNs were also investigated, and the results are given in Table 1. Interestingly, the yield of **3a** increased at first and then decreased (Table 1, entries 1–4). The maximum yield of **3a** was achieved in 90 min, and thus, this period of time was used as

Table 1 The effects of reaction time and temperature on the synthesis of **3a** photocatalyzed by p-CNNs^a


Entry	p-CNNs		Temperature (°C)	Ratio ^b	Yield ^c (%)
	dosage (wt%)	Time (min)			
1	1.12	30	40	1 : 1 : 1	14.8
2	1.12	60	40	1 : 1 : 1	19.0
3	1.12	90	40	1 : 1 : 1	26.6
4	1.12	120	40	1 : 1 : 1	25.2
5	1.12	90	30	1 : 1 : 1	17.9
6	1.12	90	50	1 : 1 : 1	48.1
7	1.12	90	70	1 : 1 : 1	72.7
8	1.12	90	90	1 : 1 : 1	84.5
9	1.12	90	100	1 : 1 : 1	82.0

^a **3a** is 5-ethoxycarbonyl-6-methyl-4-phenyl-3,4-dihydropyrimidin-2(1H)-one. ^b The order of the reactants ratio is benzaldehyde to ethyl acetoacetate to urea (5 mmol benzaldehyde, 1 equiv.). ^c Isolated yield.

the optimum reaction time for further investigations. As we know, temperature plays an important role in organic synthesis. In this study, the influence of different reaction

Table 2 The effects of p-CNNs dosage and the stoichiometric ratio of reactants on the synthesis of **3a** photocatalyzed by p-CNNs^a


Entry	p-CNNs		Temperature (°C)	Ratio	Yield ^b (%)
	dosage (wt%)	Time (min)			
1	0.56	90	90	1 : 1 : 1	75.3
2	1.12	90	90	1 : 1 : 1	84.5
3	1.68	90	90	1 : 1 : 1	88.4
4	2.80	90	90	1 : 1 : 1	87.8
5	3.92	90	90	1 : 1 : 1	87.3
6	5.60	90	90	1 : 1 : 1	80.1
7	1.68	90	90	1 : 1.2 : 1.2	84.7
8	1.68	90	90	1 : 1.2 : 1.2	94.2
9	1.68	90	90	1 : 1.2 : 1.5	95.4
10	1.68	90	90	1 : 1.5 : 1.5	68.1

^a **3a** is 5-ethoxycarbonyl-6-methyl-4-phenyl-3,4-dihydropyrimidin-2(1H)-one. ^b Isolated yield.

Table 3 Various catalysts for the synthesis of **3a** in their own appropriate reaction medium

Entry	Catalyst	Time (min)	Temperature (°C)	Solvent	Yield (%)	Ref.
1	p-CNNs (1.68 wt%)	90	90	—	95.4	This work
2	D-Xylonic acid (6.5 mol%)	300	100	D-Xylonic acid	87	2
3	ZSPS ^a (5 mol%)	30	90	—	96	41
4	SFP ^b (5 wt%)	20	100	—	94	42
5	PPH ₃ (2.78 mol%)	720	100	—	70	43
6	B(C ₆ F ₅) ₃ (2.78 mol%)	150	Reflux	EtOH	95	44
7	SBNPSA ^c (1 mol%)	240	80	EtOH	95	45
8	ZrOCl ₂ /mont K10 (40 wt%)	20	80	—	78	46

^a ZSPS represents zirconium(IV)-salophen perfluorooctanesulfonate. ^b SFP represents sulfated polyborate. ^c SBNPSA represents silica-bonded N-propyl sulfamic acid.

temperatures on the synthesis of **3a** was also explored. As the reaction temperature was increased from 30 to 90 °C, the yield of **3a** increased from 17.9 to 84.5% (Table 1, entries 3 and 5–8). However, the yield of **3a** appeared to decrease slightly when the reaction temperature was increased from 90 to 100 °C (Table 1, entries 8 and 9). This finding indicates that proper temperature is instrumental in the synthesis of **3a** in the p-CNN catalytic system irradiated by visible light.

To investigate the effects of the p-CNN photocatalyst dosage and the stoichiometry of the reactants for the synthesis of **3a**, a series of experiments was performed and the results are presented in Table 2. Firstly, the yield of **3a** increased along with the increase in the p-CNNs dosage from 0.56 to 1.68 wt% (Table 2, entries 1–3). However, no obvious increase in **3a** yield was observed when the photocatalyst dosage was 2.80, 3.92, and 5.60 wt%, respectively (Table 2, entries 4–6). This is probably because the adsorption of benzaldehyde, ethyl acetoacetate and urea on the surface of p-CNNs formed unstable species, leading to a lower activation energy of the entire reaction. Table 2 also shows the influence of the stoichiometry of the reactants on the synthesis of **3a**. Apparently, as the urea dosage increased, the yield of **3a** increased (Table 2, entries 3 and 8, 7 and 9). Conversely, the yield of **3a** decreased when the content of ethyl acetoacetate was increased (Table 2, entries 7, 8, 9 and 10). According to the aforementioned analysis, two points can be reflected. One is that the optimum reaction condition was observed at 90 °C for 90 min with the reaction ratio of 1:1.2:1.5 (benzaldehyde:ethyl acetoacetate:urea) under the irradiation of visible light with the p-CNNs photocatalyst (1.68 wt%). The other is that the Biginelli reaction for the efficient synthesis of **3a** was achieved with the assistance of photo-thermo catalysis.

To further understand the merits of the synthesis of **3a** photocatalyzed by p-CNNs, the system was compared with that of the earlier reported ones. As shown in Table 3, p-CNNs exhibited excellent activity in a shorter reaction time as compared to D-xylonic acid, PPH₃, B(C₆F₅)₃ and SBNBSA.^{2,46–48} The SFP catalyst also gave a good yield of **3a**, but suffered from the high reaction temperature.⁴⁵ SBNPSA and ZrOCl₂/mont K10 can work at relatively lower temperature and shorter time.^{48,49} However, additional solvents or metal catalysts were employed. The ZSPS catalyst exhibited excellent activity at shorter reaction time, but the catalyst preparation process is complex and expensive when compared with p-CNNs.⁴⁵ Obviously, with

respect to the efficiency or environmental economic benefit, the p-CNN system for the synthesis of **3a** is superior to most reported systems. To investigate the relationship between the structure of p-CNNs and its performance, the photocatalytic activities of ml-CN and p-CNNs on the synthesis of **3a** were investigated, and the photocatalytic performance of ml-CN was lower than that of p-CNNs. According to the characterization of SEM and AFM, the possible active sites of p-CNNs in the synthesis of **3a** was the porous structure of the p-CNNs.

To investigate the substrate universality, Biginelli reaction of various aldehydes with ethyl acetoacetate or methyl acetoacetate and urea or thiourea was performed. From the perspective of green chemistry, the stoichiometric ratio of the reactants was changed from 1:1.2:1.5 to 1:1:1.2, and the other optimum conditions were not changed. Firstly, the influences of aromatic aldehydes with different electro-donating groups and electro-withdrawing groups on the Biginelli reaction were studied. As shown in Fig. 3, excellent yields were achieved (**3b–3h**), and no obvious difference in the yields of different products was observed, indicating that the electron-donating groups and electron-withdrawing groups in the aromatic aldehyde (*p*-) are all beneficial for the Biginelli reaction. Subsequently, the effect of spatial hindrance on the Biginelli reaction was explored. The yield of the corresponding product was 90.3 (**3c**), 87.1 (**3i**) and 80.3% (**3j**) when *p*-methoxybenzaldehyde, *m*-methoxybenzaldehyde and *o*-methoxybenzaldehyde were employed, respectively. This finding suggests that larger the steric hindrance of the aromatic aldehyde, the more unfavorable the Biginelli reaction. As compared with aromatic aldehydes, fatty aldehydes used in the Biginelli reaction with ethyl acetoacetate and urea gave good yields, (**3k**, **3l**) but lower than that of the aromatic aldehydes. Furthermore, the effect of methyl

acetoacetate on the Biginelli reaction was investigated. No obvious difference in the yields of corresponding products was observed when compared with ethyl acetoacetate (**3f–3m**, **3h–3n**, **3d–3o**, **3b–3p**). In addition, the influence of thiourea on the reaction was also investigated, and 89.7% yield of **3q** was achieved. Other investigations (**3r** and **5-3a–3e**) were similar with the above ones, and all the results indicated that the photo-thermo catalysis system using p-CNNs is appropriate for the Biginelli reaction.

With regard to the excellent performance and mild reaction conditions of the reaction system, it is worth exploring for the synthesis of *N*- and *O*-heterocyclic compounds. Pyrroles and their analogs are a series of *N*-heterocyclic compounds, which play an important role in the synthesis of pharmacologically significant molecules and natural products.⁵⁰ Therefore, the synthesis of pyrroles is of great significance. In addition, benzoxanthene derivatives are a class of *O*-heterocyclic compounds. They have favorable biological and pharmaceutical properties of analgesic, antiviral and antibacterial.^{51,52} Thus, the synthesis of benzoxanthene derivatives has vital significance. For 5-phenyl-1-(4-methoxyphenyl)-3-[(4-methoxyphenyl)-amino]-1*H*-pyrrol-2(5*H*)-one synthesis, the reaction was performed at room temperature by mixing p-CNNs, benzaldehyde, 4-methoxyaniline and ethyl pyruvate in the presence of visible-light irradiation, and the yield of the product was up to 93%. However, for 12-phenyl-9,9-dimethyl-8,9,10,12-tetrahydrobenzo[*a*]xanthen-11-one synthesis, the reaction was carried out at 50 °C by mixing p-CNNs, benzaldehyde, 2-hydroxynaphthalene and 5,5-dimethyl-1,3-cyclohexanedione in the presence of visible-light irradiation, and the yield of the product was up to 97%.

Due to the excellent activity of p-CNNs, it is worth exploring its cycle stability. In this work, the cycling experiment was

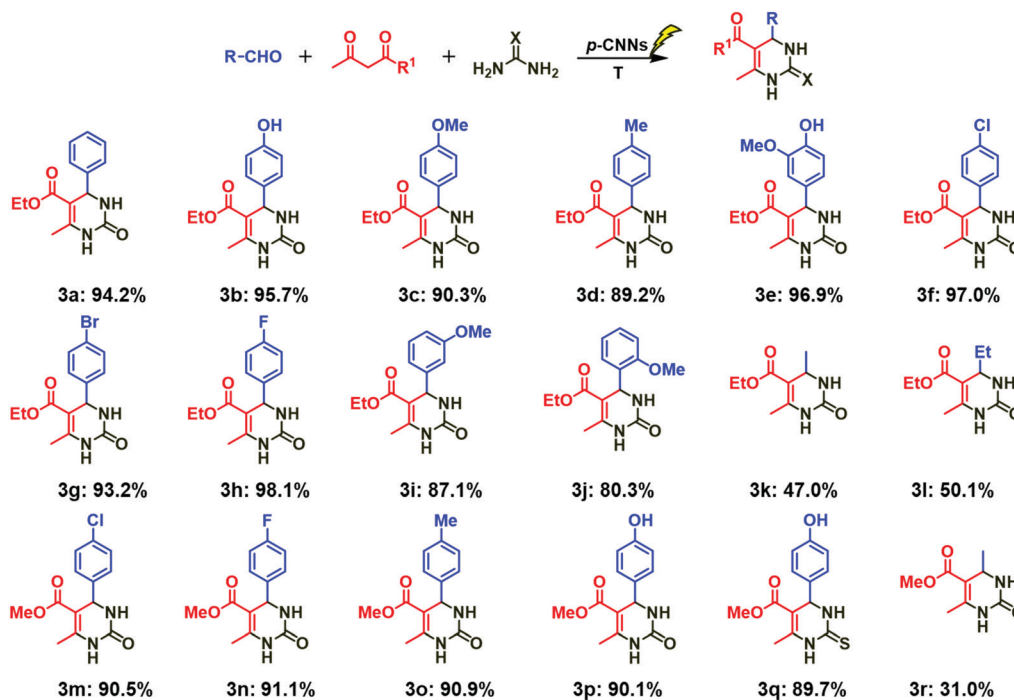


Fig. 3 Photo-thermo catalysis for the synthesis of dihydropyrimidin-2(*H*)-ones and thiones photocatalyzed by p-CNNs.

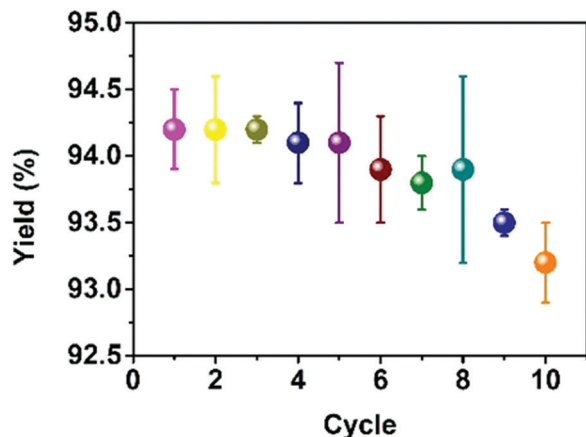


Fig. 4 Recycling of p-CNNs photocatalyst.

performed using benzaldehyde, ethyl acetoacetate and urea (1:1:1.2) at 90 °C for 90 min in the presence of p-CNNs (1.68 wt%). In the cycling experiment, the p-CNNs was recovered during the recrystallization process. The obtained p-CNNs was washed with hot ethanol several times and then dried at 100 °C for 10 h before reuse. As shown in Fig. 4, no obvious decrease in the yield of **3a** was observed, indicating that the p-CNNs has excellent stability.

Conclusions

In summary, this work provides a novel and green photocatalytic system for the synthesis of N- and O-heterocyclic compounds. The p-CNN photocatalyst showed excellent activity for the “one-pot” three-component Biginelli reaction to give DHPMs and their derivatives. The ease of use, environmental friendliness as well as air, water, and substrate tolerances make it an excellent system for carrying out Biginelli reaction. Meanwhile, 5-phenyl-1-(4-methoxyphenyl)-3-[(4-methoxyphenyl)-amino]-1H-pyrrol-2(5H)-one and 12-phenyl-9,9-dimethyl-8,9,10,12-tetrahydrobenzo[*a*]xanthen-11-one were all obtained *via* this reaction system with 93% and 97% yields, respectively, under mild reaction conditions. This work paves a novel way for the organic synthesis of heterocyclic compounds, especially the N- and O-heterocyclic compounds.

Conflicts of interest

The authors declare no conflicts of interest.

Acknowledgements

We wish to thank for the Foundation of NSFC-CONICFT Joint Project (No. 51961125207), Liaoning Province “Xingliao Talent Plan” Outstanding Talent Project (XLYC1901004), Innovation Support Program for High-level Talents of Dalian (Top and Leading Talents) (201913), National Natural Science Foundation of China (22008018), Natural Science Foundation of Liaoning Province (2020-MS-272), China Postdoctoral Science Foundation (2020M670716), Start-up Fund for Doctoral Research of Dalian

Polytechnic University (2020-07) and the Foundation (No. KF201914) of State Key Laboratory of Biobased Material and Green Papermaking, Qilu University of Technology, Shandong Academy of Sciences.

Notes and references

- C. Y. Guan, S. S. Chen, T. H. Lee, C. P. Yu and D. C. W. Tsang, *J. Cleaner Prod.*, 2020, **260**, 121097.
- J. L. Ma, L. X. Zhong, X. W. Peng and R. C. Sun, *Green Chem.*, 2016, **18**, 1738–1750.
- R. H. Mei, U. Dhawa, R. C. Samanta, W. B. Ma, D. J. Wencel and L. Ackermann, *ChemSusChem*, 2020, **13**(13), 3306–3356.
- L. Chen, D. Y. Zhu, J. T. Li, X. X. Wang, J. F. Zhu, P. S. Francis and Y. H. Zheng, *Appl. Catal., B*, 2020, **273**, 119050.
- B. Xu, G. L. Troian, R. Dykstra, R. T. Martin, O. Gutierrez and U. K. Tambar, *J. Am. Chem. Soc.*, 2020, **142**(13), 6206–6215.
- C. H. Dai and B. Liu, *Energy Environ. Sci.*, 2020, **13**, 24–52.
- S. I. G. Costa, V. D. Cauneto, F. L. D. Fiorentin, P. B. Almeida, R. C. Oliveira, E. Longo, A. N. Modenes and V. Slusarski-Santana, *Chem. Eng. J.*, 2020, **392**, 123737.
- M. Motola, M. Baudys, R. Zazpe, M. Krbal, J. Michalicka, J. Rodriguez-Pereira, D. Pavlinak, J. Prikryl, L. Hromadko, H. Sopha, J. Krysa and J. M. Macak, *Nanoscale*, 2019, **11**, 23126–23131.
- P. Zhou, Q. H. Zhang, Z. K. Xu, Q. Y. Shang, L. Wang, Y. G. Chao, Y. J. Li, H. Chen, F. Lv, Q. Zhang, L. Gu and S. J. Guo, *Adv. Mater.*, 2020, **32**, 1904249.
- A. Serra, R. Artal, A. J. Garcia, B. Sepulveda, E. Gomez, J. Nogues and L. Philippe, *Adv. Sci.*, 2019, **7**(3), 1902447.
- E. Bardos, A. K. Kiraly, Z. Pap, L. Baia, S. Garg and K. Hernadi, *Appl. Surf. Sci.*, 2019, **479**, 745–756.
- M. L. Luo, Q. Yang, W. B. Yang, J. H. Wang, F. F. He, K. W. Liu, H. M. Cao and H. J. Yan, *Small*, 2020, **16**(20), 2001100.
- L. Qin, R. Ru, J. W. Mao, Q. Meng, Z. Fan, X. Li and G. L. Zhang, *Appl. Catal., B*, 2020, **269**, 118754.
- L. W. Zhang, R. Long, Y. M. Zhang, D. L. Duan, Y. J. Xiong, Y. J. Zhang and Y. P. Bi, *Angew. Chem., Int. Ed.*, 2020, **59**(15), 6224–6229.
- X. W. Zhu, J. M. Yang, X. J. She, Y. H. Song, J. C. Qian, Y. Wang, H. Xu, H. M. Li and Q. Y. Yan, *J. Mater. Chem. A*, 2019, **7**(10), 5209–5213.
- C. K. Yao, A. L. Yuan, Z. S. Wang, H. Lei, L. Zhang, L. M. Guo and X. P. Dong, *J. Mater. Chem. A*, 2019, **7**(21), 13071–13079.
- F. He, B. C. Zhu, B. Cheng, J. G. Yu, W. K. Ho and W. Macyk, *Appl. Catal., B*, 2020, **272**, 119006.
- X. W. Zhu, S. Q. Huang, Q. Yu, Y. B. She, J. M. Yang, G. L. Zhou, Q. D. Li, X. J. She, J. J. Deng, H. M. Li and H. Xu, *Appl. Catal., B*, 2020, **269**, 118760.
- Z. S. Wang, H. J. Yu, L. Zhang, L. M. Guo and X. P. J. Dong, *J. Taiwan Inst. Chem. Eng.*, 2020, **107**, 119–128.
- X. L. Xue, R. P. Chen, C. Z. Yan, Y. Hu, W. J. Zhang, S. Y. Yang, L. B. Ma, G. Y. Zhu and Z. Jin, *Nanoscale*, 2019, **11**, 10439–10445.

- 21 X. J. Wu, X. T. Fan, S. J. Xie, J. C. Lin, J. Cheng, Q. H. Zhang, L. Y. Chen and Y. Wang, *Nat. Catal.*, 2018, **1**, 772–780.
- 22 S. Cailotto, M. Negrato, S. Daniele, R. Luque, M. Selva, E. Amadio and A. Perosa, *Green Chem.*, 2020, **22**, 1145–1149.
- 23 C. O. Kappe, *Mol.*, 1998, **3**(1), 1–9.
- 24 C. O. Kappe, *Eur. J. Med. Chem.*, 2000, **35**, 1043–1052.
- 25 M. Kidwai, S. Saxena, M. K. R. Khan and S. S. Thukral, *Eur. J. Med. Chem.*, 2005, **40**(8), 816–819.
- 26 K. S. Atwal, G. C. Rovnyak, S. D. Kimball, D. M. Floyd, S. Moreland, B. N. Swanson, J. Z. Gougoutas, J. Schwartz, K. M. Smillie and M. F. Malley, *J. Med. Chem.*, 1990, **33**(9), 2629–2635.
- 27 K. S. Atwal, B. N. Swanson, S. E. Unger, D. M. Floyd, S. Moreland, A. Hedberg and B. C. O'Reilly, *J. Med. Chem.*, 1991, **34**, 806–811.
- 28 B. B. Snider and Z. Shi, *J. Org. Chem.*, 1993, **58**, 3828–3839.
- 29 A. D. Patil, N. V. Kumar, W. C. Kokke, M. F. Bean, A. J. Freyer, C. Debrosse, S. Mai, A. Truneh, D. J. Faulkner, B. Carte, A. L. Breen, R. P. Hertzberg, R. K. Johnson, J. W. Westley and B. C. M. Potts, *J. Org. Chem.*, 1995, **60**(5), 1182–1188.
- 30 P. Biginelli, *Ital.*, 1893, **23**, 360–416.
- 31 K. S. Atwal, G. C. Rovnyak, B. C. O'Reilly and J. Schwartz, *J. Org. Chem.*, 1989, **54**, 5898–5907.
- 32 B. Jauk, F. Belaj and C. O. Kappe, *J. Chem. Soc., Perkin Trans. 1*, 1999, 307–314.
- 33 N. A. Liberto, S. d. P. Silva, A. de Fatima and S. A. Fernandes, *Tetrahedron*, 2013, **69**, 8245–8249.
- 34 W. Su, J. J. Li, Z. G. Zheng and Y. C. Shen, *Tetrahedron Lett.*, 2005, **46**, 6037–6040.
- 35 J. Safari and Z. Zarnegar, *New J. Chem.*, 2014, **38**, 358–365.
- 36 M. K. Raj, H. S. P. Rao, S. GManjunatha, R. Sridharan, S. Nambiar, J. Keshwan, J. Rappai, S. Bhagat, B. S. Shwetha, D. Hegde and U. Santhosh, *Tetrahedron Lett.*, 2011, **52**(28), 3605–3609.
- 37 A. de Vasconcelos, P. S. Oliveira, M. Ritter, R. A. Freitag, R. L. Romano, F. H. Quina, L. Pizzuti, C. M. P. Pereira, F. M. Stefanello and A. G. Barschak, *J. Biochem. Mol. Toxicol.*, 2012, **26**(4), 155–161.
- 38 C. Jiang and Q. D. You, *Chin. Chem. Lett.*, 2007, **18**(6), 647–650.
- 39 Q. Zhang, X. Wang, Z. Li, W. Wu, J. Liu, H. Wu, S. Cui and K. Guo, *RSC Adv.*, 2014, **4**, 19710–19715.
- 40 X. C. Wang, K. Maeda, A. Thomas, K. Takanabe, G. Xin, J. M. Carlsson, K. Domen and M. Antonietti, *Nat. Mater.*, 2009, **8**(1), 76–80.
- 41 J. W. Fu, B. C. Zhu, C. J. Jiang, B. Cheng, W. You and J. G. Yu, *Small*, 2017, **13**(15), 1603938.
- 42 Q. D. Qin, X. Gao, X. Wu and Y. H. Liu, *Mater. Lett.*, 2019, **256**, 126623.
- 43 Q. Liu, T. X. Chen, Y. R. Guo, Z. G. Zhang and X. M. Fang, *Appl. Catal., B*, 2017, **205**, 173–181.
- 44 N. B. Li, Y. J. Wang, F. J. Liu, X. Zhao, X. H. Xu, Q. An and K. M. Yun, *Appl. Organomet. Chem.*, 2020, **34**(3), e5454.
- 45 C. K. Khatri, D. S. Rekunge and G. U. Chaturbhuji, *New J. Chem.*, 2016, **40**(12), 10412–10417.
- 46 H. Slimi, Y. Moussaoui and R. ben Salem, *Arabian J. Chem.*, 2016, **9**, 510–514.
- 47 S. K. Prajapati, K. K. Gupta and B. N. Babu, *J. Chem. Sci.*, 2015, **127**(6), 1047–1052.
- 48 S. R. Jetti, A. Bhatewara, T. Kadre and S. Jain, *Chin. Chem. Lett.*, 2014, **25**(3), 469–473.
- 49 B. Vijayakumar and G. R. Rao, *J. Porous Mater.*, 2012, **19**(4), 491–497.
- 50 N. R. Candeias, P. M. P. Gois and C. A. M. Afonso, *J. Org. Chem.*, 2006, **71**(15), 5489–5497.
- 51 H. N. Hafez and M. I. Hegab, *Bioorg. Med. Chem. Lett.*, 2008, **18**(16), 4538–4543.
- 52 H. Wang, L. Lu, S. Y. Zhu, Y. H. Li and W. M. Cai, *Curr. Microbiol.*, 2006, **52**(1), 1–5.